Available online at www.sciencedirect.com
ScienceDirect
Information Sciences 177 (2007) 1999–2022
INFORMATION SCIENCES
AN INTERNATIONAL JOURNAL
www.elsevier.com/locate/ins

# Combining fuzzy, PID and regulation control for an autonomous mini-helicopter

Edgar N. Sanchez [a], Hector M. Becerra [a,*], Carlos M. Velez [b]

[a] *CINVESTAV, Unidad Guadalajara, Apartado Postal 31-438, Plaza la Luna, Guadalajara, Jalisco CP 45091, Mexico*
[b] *Universidad EAFIT, Carrera 49, No. 7, Sur 50. Medellin, Colombia*

Received 19 September 2006; accepted 6 October 2006

**Abstract**

This paper reports on the synthesis of different flight controllers for an X-Cell mini-helicopter. They are developed on the basis of the most realistic mathematical model currently available. Two hybrid intelligent control systems, combining computational intelligence methodologies with other control techniques, are investigated. For both systems, Mamdani-type fuzzy controllers determine the set points for altitude/attitude control. These fuzzy controllers are designed using a simple rule base. The first scheme consists of conventional SISO PID controllers for $z$-position and roll, pitch and yaw angles. In the second scheme, two of the previous PID controllers are used for roll and pitch, and a linear regulator is added to control altitude and yaw angle. These control schemes mimic the action of an expert pilot. The designed controllers are tested via simulations. It is shown that the designed controllers exhibit good performance for hover flight and control positioning at slow speed.


*Keywords:* Mamdani-type fuzzy control; Linear regulation; PID control; Hybrid intelligent control; Autonomous helicopter

## 1. Introduction

The research reported in this paper is a contribution to the overall objective of the Colibri project [19]: the design and implementation of, and experimentation on, a control system for a mini-helicopter robot. The Colibri project is one of the most important research projects under development in Colombia, South America. There already exist some publications on intelligent and hybrid intelligent control [5] for aircrafts and helicopters [4,10,13–15,18]. Digressing from this work, this paper proposes a new hybrid intelligent approach, which combines fuzzy, PID and regulation control. The viability of this new approach is illustrated by its application to a mini-helicopter robot.

* Corresponding author.
*E-mail addresses:* sanchez@gdl.cinvestav.mx (E.N. Sanchez), bhecerra@gmaill.com (H.M. Becerra), cmvelez@eafit.edu.co (C.M. Velez).

0020-0255/$ - see front matter 
doi:10.1016/j.ins.2006.10.001

Helicopter control requires first, guaranteed stability at different points, to hold the helicopter in a desired trim state; and second, a method changing the helicopter velocity, position and orientation in order to track a desired trajectory. In mini-helicopters, this is usually done through a remote control system by a human pilot.

The particular problem addressed in this paper concerns the synthesis of control structures to reproduce the pilot action in its simplest form, by means of a fuzzy controller, which uses the minimum possible number of rules. Thus, an altitude and attitude (roll, pitch, and yaw) controller, which achieves stable behavior for an unmanned helicopter, must be designed. The flight control structures proposed in this paper use a nonlinear multiple-input–multiple-output (MIMO) model of a real unmanned helicopter platform, the X-Cell, via numerical simulations. The simulation model is implemented on the basis of the mathematical model proposed in [3], which is the most realistic model currently available for this mini-helicopter.

The paper is organized as follows. Section 2 briefly introduces the mini-helicopter mathematical model. Section 3 presents the general control structure. Section 4 discusses the development and performance of the first hybrid intelligent control system, which combines fuzzy and PID control theory. Section 5 describes the design of a linear regulator, which is added to the previous control system. Finally, Section 6 provides relevant conclusions.

## 2. Mathematical model

The platform for research is an X-Cell mini-helicopter, which is shown in Fig. 1. This helicopter is part of the Colibri project. The X-Cell mini-helicopter is a representative vehicle for modern research. It is highly maneuverable as a result from its stiff rotor head, allowing the transmission of large control moments from the rotor to the fuselage, a large thrust-to-weight ratio, and a fast rotor speed. This helicopter is equipped with a powerful engine and an electronic governor to maintain a nearly constant rotor speed. Like most miniature helicopters, it is also equipped with a stabilizer bar, which acts as a lagged attitude rate feedback, and is designed to help the remote human pilot to control attitude dynamics. As part of the Colibri project, an X-Cell helicopter is being instrumented to perform autonomous flight in real time.

The X-Cell mathematical model is based on [3]. This model has seventeen state variables. Among them, several parameters must be estimated experimentally and others are measured directly. The model covers from hover to about 20 m/s forward flight (low advance ratio $\leqslant 0.15$). This permits to consider that thrust is perpendicular to the rotor disk.

### 2.1. Rigid-body equations of motion

The helicopter is a vehicle that is free to simultaneously rotate and translate in all six degrees of freedom (DOF), which are: rolling, pitching, yawing, surging, swaying and heaving. The rigid-body dynamics of such vehicles are described by the Newton–Euler equations of motion. There exist two reference frames which are generally used to determine the motion of a helicopter: the body-fixed framework and the inertial framework. The equations of motion with respect to the body-fixed reference frame are

Fig. 1. X-Cell mini-helicopter.

$$m\dot{\upsilon} + m(\omega \times \upsilon) = \mathbf{F} \tag{1}$$

$$\mathbf{I}\dot{\omega} + (\omega \times \mathbf{I}\omega) = \mathbf{M} \tag{2}$$

where $\upsilon = [u \quad v \quad w]^{\mathrm{T}}$ is the vector of body velocities, $\omega = [p \quad q \quad r]^{\mathrm{T}}$ is the vector of angular rates, $\mathbf{F} = [X \quad Y \quad Z]^{\mathrm{T}}$ is the vector of external forces acting on the vehicle's center of gravity (c.g.), $\mathbf{M} = [L \quad M \quad N]^{\mathrm{T}}$ is the vector of external moments, $m$ is the helicopter mass, and $\mathbf{I}$ is the inertial tensor. The external forces and moments are produced by the main and tail rotors, the gravitational forces, and the aerodynamic forces created by the fuselage and the tail surfaces. The strongest force is due to the main rotor.

Three differential equations describing the helicopter translational motion (3) about its three body-fixed reference axes, with the origin at the vehicle's center of gravity, are derived from (1), as follows:

$$\begin{aligned}
\dot{u} &= vr - wq - g\sin\theta + (X_{\mathrm{mr}} + X_{\mathrm{fus}})/m \\
\dot{v} &= wp - ur + g\sin\phi\cos\theta + (Y_{\mathrm{mr}} + Y_{\mathrm{fus}} + Y_{\mathrm{tr}} + Y_{\mathrm{vf}})/m \\
\dot{w} &= uq - vp + g\cos\phi\cos\theta + (Z_{\mathrm{mr}} + Z_{\mathrm{fus}} + Z_{\mathrm{ht}})/m
\end{aligned} \tag{3}$$

where $\phi$ is the roll angle, $\theta$ is the pitch angle, and $g$ is the gravity acceleration. Similarly, from Eq. (2), the following three ordinary differential equations describing the helicopter rotational motion (4), are derived (note that these equations do not depend on the reference frame):

$$\begin{aligned}
\dot{p} &= \frac{(I_{yy} - I_{zz})I_{zz} - I_{xz}^2}{I_{xx}I_{zz} - I_{xz}^2}qr + \frac{(I_{xx} - I_{yy} + I_{zz})I_{xz}}{I_{xx}I_{zz} - I_{xz}^2}pq + \frac{I_{zz}}{I_{xx}I_{zz} - I_{xz}^2}L + \frac{I_{xz}}{I_{xx}I_{zz} - I_{xz}^2}N \\
\dot{q} &= \frac{I_{zz} - I_{xx}}{I_{yy}}pr - \frac{I_{xz}}{I_{yy}}\left(p^2 - r^2\right) + \frac{1}{I_{yy}}M \\
\dot{r} &= \frac{(I_{xx} - I_{yy})I_{xx} - I_{xz}^2}{I_{xx}I_{zz} - I_{xz}^2}pq + \frac{(I_{xx} - I_{yy} + I_{zz})I_{xz}}{I_{xx}I_{zz} - I_{xz}^2}qr + \frac{I_{xz}}{I_{xx}I_{zz} - I_{xz}^2}L + \frac{I_{xx}}{I_{xx}I_{zz} - I_{xz}^2}N
\end{aligned} \tag{4}$$

where $L = L_{\mathrm{mr}} + L_{\mathrm{vf}} + L_{\mathrm{tr}}$, $M = M_{\mathrm{mr}} + M_{\mathrm{ht}}$, and $N = -Q_{\mathrm{e}} + N_{\mathrm{vf}} + N_{\mathrm{tr}}$. The subscript refers to the component generating the respective force or moment: main rotor (mr), tail rotor (tr), fuselage (fus), and the stabilizers; vertical fin (vf) and horizontal tail (ht). $Q_{\mathrm{e}}$ is the torque produced by the engine to counteract the aerodynamic torque on the main rotor blades. For the above equations, we assumed that the fuselage center of pressure coincides with the c.g.; therefore, the moments created by the fuselage aerodynamic forces are neglected. See [3] for details about force and moment expressions.

The six previous first-order differential equations constitute the rigid-body equations. We can calculate the inertial position $(x, y, z)$ and the Euler angles $(\phi, \theta, \psi)$ from them, using suitable transformations. Euler angles give information about attitude.

Solving the following three differential equations provides the inertial position from body velocities:

$$\begin{bmatrix} \dot{x} \\ \dot{y} \\ \dot{z} \end{bmatrix} = \mathbf{R} \begin{bmatrix} u \\ v \\ w \end{bmatrix} \tag{5}$$

$$R = \begin{bmatrix} \mathrm{c}\theta\mathrm{c}\psi & \mathrm{s}\phi\mathrm{s}\theta\mathrm{c}\psi - \mathrm{c}\phi\mathrm{s}\psi & \mathrm{c}\phi\mathrm{s}\theta\mathrm{c}\psi + \mathrm{s}\phi\mathrm{s}\psi \\ \mathrm{c}\theta\mathrm{s}\psi & \mathrm{s}\phi\mathrm{s}\theta\mathrm{s}\psi + \mathrm{c}\phi\mathrm{c}\psi & \mathrm{c}\phi\mathrm{s}\theta\mathrm{s}\psi - \mathrm{s}\phi\mathrm{c}\psi \\ -\mathrm{s}\theta & \mathrm{s}\phi\mathrm{c}\theta & \mathrm{c}\phi\mathrm{c}\theta \end{bmatrix} \tag{6}$$

where $\mathbf{R}$ is the transformation from body-fixed to inertial reference frame, and $\mathrm{c}\theta$ and $\mathrm{s}\theta$ represent $\cos\theta$ and $\sin\theta$, respectively. The rotation matrix $\mathbf{R}$ has the following important properties:

- It can be described by the product of individual rotation matrices.
- It is an orthogonal matrix.
- Its determinant is unity.

Finally, to determine the Euler angles from angular rates, we use the following transformation:

$$\begin{bmatrix} \dot{\phi} \\ \dot{\theta} \\ \dot{\psi} \end{bmatrix} = \begin{bmatrix} 1 & \mathrm{t}\theta\mathrm{s}\phi & \mathrm{t}\theta\mathrm{c}\phi \\ 0 & \mathrm{c}\phi & -\mathrm{s}\phi \\ 0 & \mathrm{s}\phi/\mathrm{c}\theta & \mathrm{c}\phi/\mathrm{c}\theta \end{bmatrix} \begin{bmatrix} p \\ q \\ r \end{bmatrix} \tag{7}$$

### 2.2. Extension of the rigid-body model

To improve the rigid-body model accuracy, higher-order effects are taken into account, which are coupled to the rigid-body dynamics. These extensions are rotor dynamics, and engine-drive train and actuator dynamics. The former are critical because on the X-Cell the main rotor, forces and moments largely dominate the dynamic response. The coupled rotor and stabilizer bar equations are lumped into one first-order equation of motion. This procedure is carried out for both lateral ($b_1$) and longitudinal ($a_1$) flapping angles, according to the tip-path-plane rotor model [11]. The equations are expressed in the form

$$\begin{aligned} \dot{b}_1 &= -p - \frac{b_1}{\tau_e} - \frac{1}{\tau_e}\frac{\partial b_1}{\partial \mu_v}\frac{v - v_w}{\Omega R} + \frac{B_{\delta_{lat}}}{\tau_e}\delta_{lat} \\ \dot{a}_1 &= -q - \frac{a_1}{\tau_e} - \frac{1}{\tau_e}\left(\frac{\partial a_1}{\partial \mu}\frac{u - u_w}{\Omega R} + \frac{\partial a_1}{\partial \mu_z}\frac{w - w_w}{\Omega R}\right) + \frac{A_{\delta_{lon}}}{\tau_e}\delta_{lon} \end{aligned} \tag{8}$$

where $B_{\delta_{lat}}$ and $A_{\delta_{lon}}$ are effective steady-state lateral and longitudinal gains from the cyclic inputs to the main rotor flapping angles; $\delta_{lat}$ and $\delta_{lon}$ are the lateral and longitudinal cyclic control inputs; $u_w$, $v_w$ and $w_w$ are the wind components along, respectively, $X$, $Y$ and $Z$ helicopter body axes; and $\tau_e$ is the effective rotor time constant for a rotor with a stabilizer bar. The partial derivatives are approximated by a set of functions that are determined experimentally. See [3] for details.

The other inputs, $\delta_{col}$ and $\delta_{ped}$, do not explicitly appear in any equation shown in this paper, but are used for the computation of main and tail rotor thrust ($T_{mr}$ and $T_{tr}$, respectively). This involves an iterative computation of the thrust coefficients, which are included in the simulation model.

The rotor speed dynamics are also modeled, including an electronic governor, which regulates rotor speed by changing the throttle. It is worth noting that the rotor speed is not constant; it is included in the dynamics as proposed in [3].

Actuators are accurately modeled as third-order transfer functions for the collective and cyclic (lateral and longitudinal) inputs. A second-order transfer function is used for the pedals input. No inflow dynamics are necessary, because the settling time for the inflow is significantly faster than the rigid-body dynamics.

Eqs. (3), (4), (5), (7) and (8) constitute the mathematical model for the X-Cell. The rotational kinematic equation (7) are calculated using quaternions (four differential equations). Therefore, fifteen state variables are included in Eqs. (3), (4), (5), (7), (8). By adding one state for rotor speed and one state for the rotor speed tracking error, the overall model has seventeen state variables. This mathematical model is implemented in Matlab/Simulink, which is a trademark of The MathWorks Inc. For our simulations, the fuel consumption is kept constant and the total mass ($m$) is assumed to decrease with time.

## 3. General control structure

Various types of control modes have already been tested for an unmanned helicopter [6,8,11,16]. Each control mode is named according to the states variables that are considered outputs. For example, to keep the helicopter at a specific location, the position and heading ($x, y, z, \psi$) control mode is used. For a sensor failure, such as the absence of position information from the global positioning system (GPS), altitude and attitude ($z, \phi, \theta, \psi$) control mode is more desirable to stabilize the vehicle, since the on-board inertial navigation system (INS) would still be able to provide altitude and attitude information. The set of outputs $x$, $y$, $z$, $\beta$, constitutes the position and side slip angle mode. In particular, if the controller tries to keep slide slip angle, $\beta$, at values near zero, the system is said to be operated in coordinated flight mode.

The X-Cell helicopter is equipped with a remote control operated by a human pilot to maintain the desired attitude. As with any VTOL vehicle, it is maneuvered by controlling its attitude angles. The objective of the present paper is to substitute the action of a pilot for an on-board automatic control system, using an altitude/attitude control mode strategy. Hence, we can move the helicopter to a specific location by tilting it adequately, such that the rotor produces sufficiently large horizontal forces. The larger the pitch or roll angle, the bigger the longitudinal, respectively lateral, propulsive force.

Fig. 2 shows the general control structure proposed. It consists of two control loops; the inner loop controls the faster dynamics (altitude and attitude), whilst the outer loop controls the slower dynamics (lateral and longitudinal translation).

As can be seen in this diagram, four inputs are used as references for the desired tri-dimensional position and yaw angle $(x^{\mathrm{d}}, y^{\mathrm{d}}, z^{\mathrm{d}}, \psi^{\mathrm{d}})$. The lateral/longitudinal control is carried by two Mamdani-type fuzzy controllers, and for the altitude/attitude control, the first scheme uses PID controllers, and the second one combines PID and regulation control. According to the control technique used for the altitude/attitude controller, the inner loop requires more or less variables for feedback. The PID controllers require only $z$, $\phi$, $\theta$ and $\psi$, whereas the linear regulator requires $v_z$, $p$, $q$, $r$, $a_1$ and $b_1$.

The synthesis procedure is carried out sequentially. First, it is necessary to ensure attitude control, then translational control. An altitude/attitude control mode allows the helicopter to be controlled almost as by a human pilot. The helicopter attitude dynamics are conditionally stable, which means that a minimum amount of attitude feedback is required for the system to be stable. However, excessive feedback will destabilize the system [11].

## 4. Combining fuzzy and PID control

Based on the above main control objectives, we designed the altitude/attitude control using SISO PID controllers. The lateral/longitudinal control is constituted by two Mamdani-type fuzzy controllers.

### 4.1. PID controllers

The scheme in Fig. 3 is composed of four independent PID controllers, one for each angle $(\phi, \theta, \psi)$ and one for altitude $(z)$. The PID controllers present good performance for many real world applications [1], and to control a helicopter, they are suitable for providing the minimum amount of feedback to stabilize the handled variables. The maximum actuators ranges must be considered, in order to avoid saturation.

Tuning is difficult due to the strong coupling between the state variables. The four PID controllers have to be tuned at the same time. Initially, introducing adequate proportional feedback in all the loops is sufficient to stabilize the attitude angles and to force the $z$-position close to the desired value. At the beginning, it is important to find suitable gains for the altitude and yaw controllers, while keeping small gains for the other two controllers. Once a stable dynamics is achieved, the proportional gains have to be increased to reduce offset. However, offset is only eliminated by including the integral part, with a small gain to avoid instability. It is necessary to add a derivative part to improve stability and to increase the integral gains, and therefore, to obtain a well-behaved performance for each variable. Finally, all the controllers have proportional, integral and derivative components, whose gains are tuned by trial and error. It is worth noting that it is not easy

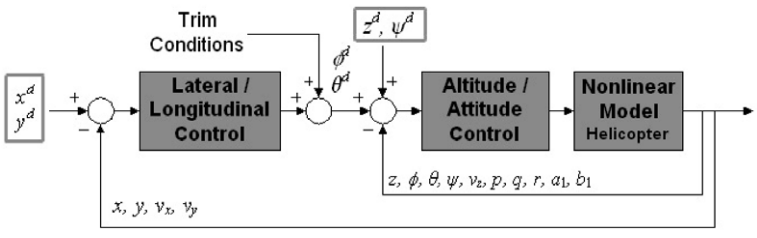


Fig. 2. General control structure.

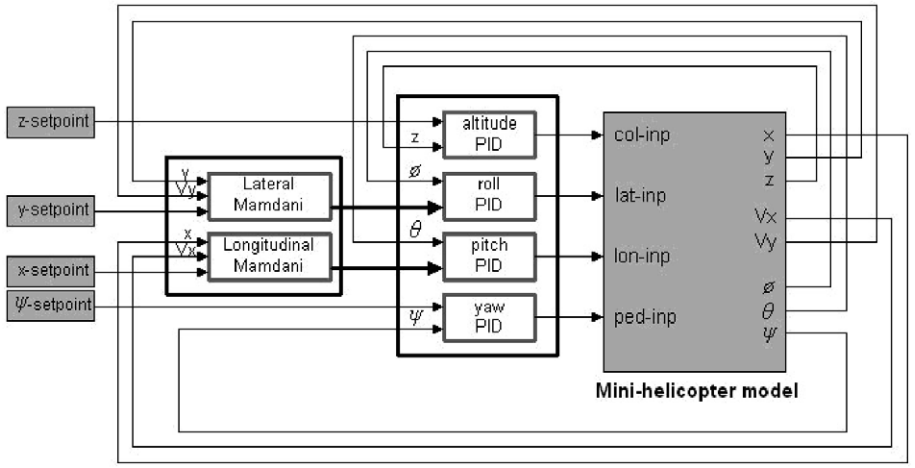


Fig. 3. Detailed scheme for combining fuzzy and PID control.

to obtain good results; we ensure them by fulfilling criteria such as setting time (<20 s), overshoot (<20%) and steady-state error (<1%). Even so, the whole procedure is completely experimental.

**Comment 1.** Due to the very strong coupling effects, it not possible to use any of the well-known PID tuning procedures. For this reason, we follow the experimental procedure explained in the previous paragraph.

The transfer function considered for each PID controller is as follows:

$$\frac{C(s)}{U(s)} = K_p + \frac{K_i}{s} + K_d s \tag{9}$$

The selected gains used for each controller are shown in Table 1.

### 4.2. Lateral/longitudinal control

We use Mamdani-type fuzzy controllers to control $x$, $y$ position. This type of controller has a heuristic nature [12,17], which reflects the experience of a human pilot.

A key issue in the design of the Mamdani-type fuzzy controllers is the trim conditions. A helicopter is said to be at trim if all of the aerodynamic and gravitational forces, and aerodynamic moments acting on the helicopter about its center of gravity, are in balance. It is worth noting that the system trim conditions do not depend on positions, velocities and yaw. A detailed explanation of the trim conditions calculation is presented in [8]. Six values are obtained as trim conditions: $\delta_{\text{col}}^{\text{T}}$, $\delta_{\text{ped}}^{\text{T}}$, $a_1^{\text{T}}$, $b_1^{\text{T}}$, $\theta^{\text{T}}$ and $\phi^{\text{T}}$. In our case, it is important to know the last two conditions, because these values allow us to obtain lateral and longitudinal steady-state positions.

To compute the trim condition, it is necessary to approximate the expressions for the total force and total moment (given in [3]), without considering contribution of the stabilizers. This is possible because the contribution of stabilizers on the total force and total moment is small. Moreover, an approximation of the rotor

Table 1
Gain values for each PID controller

| | $K_p$ | $K_i$ | $K_d$ |
|---|---|---|---|
| Altitude-PID | 3 | 0.2 | 0.6 |
| Roll-PID | 3 | 0.5 | 0.2 |
| Pitch-PD | 3 | 1 | 0.2 |
| Yaw-PID | 10 | 1.5 | 10 |

thrust is made for solving the trim condition. As a result of this computation, the attitude trim, in radians, is $\phi^{\mathrm{T}} = 0.074665$ and $\theta^{\mathrm{T}} = 0$. The real attitude trim used in the simulations is $\phi^{\mathrm{T}} = 0.07988$ and $\theta^{\mathrm{T}} = 0$ in radians.

Finally, two Mamdani controllers were designed to adequately determine roll and pitch angle reference values, according to the signs definition presented in Fig. 4. Both controllers were designed to be as simple as possible.

1. *Fuzzy representation*: Fig. 5 displays the input membership functions for the Mamdani controllers. Three membership functions were used for each input, corresponding to negative, zero or positive values of position error and velocity.

Fig. 6 presents the output membership functions used for the Mamdani controllers. One membership function is used for each rule. The labels for each output membership function are from $s_1$ to $s_9$, representing the possible values for pitch and roll, as shown in the horizontal axis of Fig. 6. For example, $s_1$ represents the biggest negative value, $s_9$ the biggest positive value, and $s_5$ is the membership function for zero output.

2. *Mamdani rules for lateral position*: Given a reference $y$-position, $y_{\mathrm{d}}$, this controller infers a desired roll angle, $\phi_{\mathrm{d}}$, using $y$-position error, $e_y = y - y_{\mathrm{d}}$, and velocity, $v_y$. Both inputs to the lateral Mamdani controller are in inertial reference frame. The nine rules used to compute the desired value for the desired roll angle are

**If** $e_y$ is Neg and $v_y$ is Neg, **Then** $\phi_{\mathrm{d}}$ is $s_9$
**If** $e_y$ is Zero and $v_y$ is Neg, **Then** $\phi_{\mathrm{d}}$ is $s_8$
**If** $e_y$ is Pos and $v_y$ is Neg, **Then** $\phi_{\mathrm{d}}$ is $s_7$
**If** $e_y$ is Neg and $v_y$ is Zero, **Then** $\phi_{\mathrm{d}}$ is $s_6$
**If** $e_y$ is Zero and $v_y$ is Zero, **Then** $\phi_{\mathrm{d}}$ is $s_5$
**If** $e_y$ is Pos and $v_y$ is Zero, **Then** $\phi_{\mathrm{d}}$ is $s_4$
**If** $e_y$ is Neg and $v_y$ is Pos, **Then** $\phi_{\mathrm{d}}$ is $s_3$
**If** $e_y$ is Zero and $v_y$ is Pos, **Then** $\phi_{\mathrm{d}}$ is $s_2$
**If** $e_y$ is Pos and $v_y$ is Pos, **Then** $\phi_{\mathrm{d}}$ is $s_1$

These rules are derived heuristically. The interpretation of the first rule is as follows: if the position error is negative and its rate of change is also negative, (the helicopter is moving away from the desired position, which is caused by a negative roll angle), then, a positive, relatively big roll angle is required, in order to slow down the lateral motion, reverse the velocity and reduce the position error. All the other rules can be similarly explained.

3. *Mamdani rules for longitudinal position*: Given a reference $x$-position, $x_{\mathrm{d}}$, this controller infers a desired pitch angle, $\theta_{\mathrm{d}}$, using an $x$-position error, $e_x = x - x_{\mathrm{d}}$, and a velocity, $v_x$. Both inputs to the longitudinal Mamdani controller are in an inertial reference frame. The analogous nine rules used to compute the desired value for the desired pitch angle are:

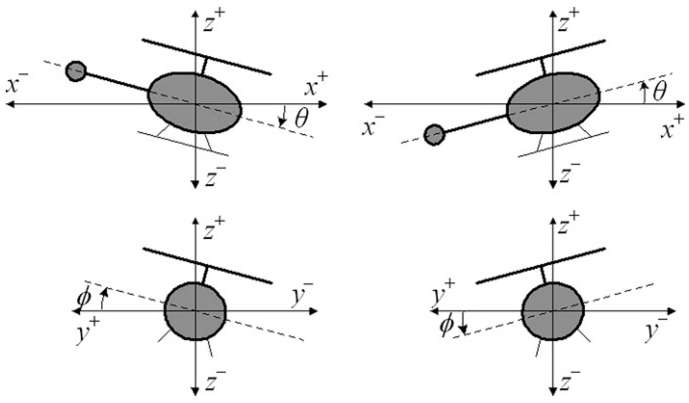


Fig. 4. Signs definition for the variables involved in lateral/longitudinal motion.

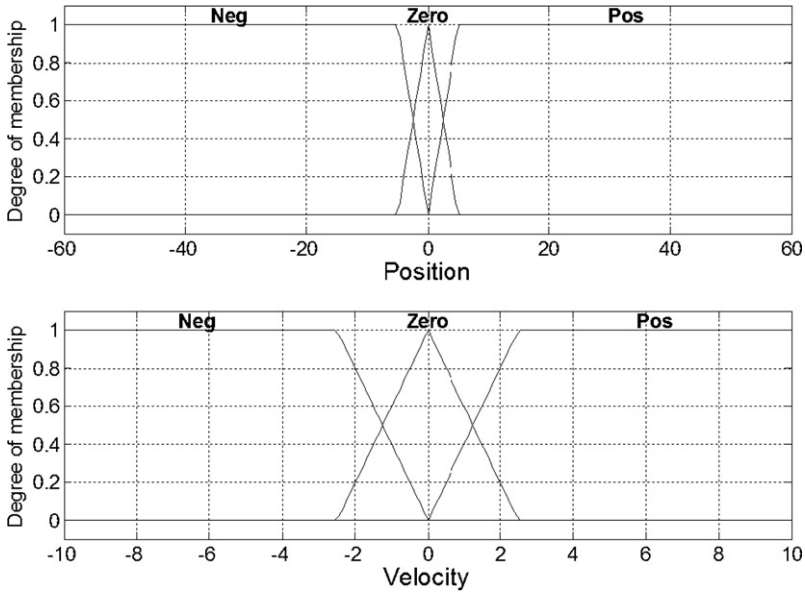


Fig. 5. Input membership functions used for each fuzzy controller.

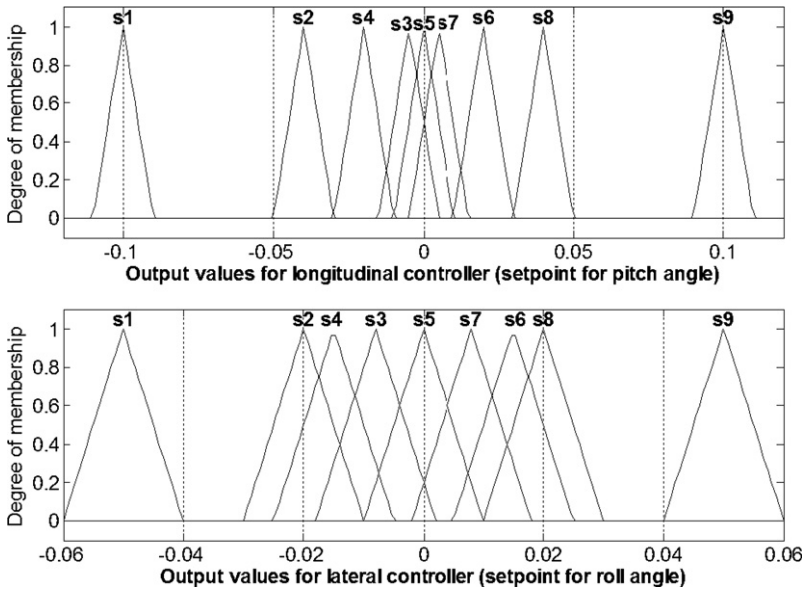


Fig. 6. Output membership functions used for each fuzzy controller.

**If** $e_x$ is Neg and $v_x$ is Neg, **Then** $\theta_d$ is $s_1$
**If** $e_x$ is Zero and $v_x$ is Neg, **Then** $\theta_d$ is $s_2$
**If** $e_x$ is Pos and $v_x$ is Neg, **Then** $\theta_d$ is $s_3$
**If** $e_x$ is Neg and $v_x$ is Zero, **Then** $\theta_d$ is $s_4$
**If** $e_x$ is Zero and $v_x$ is Zero, **Then** $\theta_d$ is $s_5$
**If** $e_x$ is Pos and $v_x$ is Zero, **Then** $\theta_d$ is $s_6$
**If** $e_x$ is Neg and $v_x$ is Pos, **Then** $\theta_d$ is $s_7$
**If** $e_x$ is Zero and $v_x$ is Pos, **Then** $\theta_d$ is $s_8$
**If** $e_x$ is Pos and $v_x$ is Pos, **Then** $\theta_d$ is $s_9$

These rules are derived heuristically. As an example, the interpretation of the first rule is as follows: if the position error is negative and its rate of change is also negative, (the helicopter is moving away from the desired position, which is caused by a positive pitch angle), then, a negative, relatively big pitch angle is required in order to slow down the longitudinal motion, reverse the velocity and reduce the position error. All the other rules can be similarly explained.

To illustrate the performance of one of these Mamdani-type fuzzy controller, the following response is calculated by the longitudinal one: if the helicopter is positioned 3.5 m behind its $x$-reference, and the position error is increasing with a velocity of 1.65 m/s, then the longitudinal controller infers that a -0.0588 rad pitch angle is required to return the vehicle toward the desired position.

**Comment 2.** The Mamdani fuzzy approach is selected, instead of the Takagi–Sugeno approach, because: (a) it allows for the inclusion of experimental knowledge for the controller synthesis, such as that from the flight of the mini-helicopter by a human pilot, (b) it does not require a mathematical model of the mini-helicopter, and (c) it deals with the aforementioned coupling effects. To apply the Takagi–Sugeno fuzzy approach to the whole system is impractical because important nonlinear effects would not be considered, even using many local linear models.

### 4.3. Simulation results

In this section, we discuss the performance of the control scheme that combines fuzzy and PID control. The PID controllers' performance is presented by tracking a square signal for each attitude angle independently. First, it is illustrated how the overall control system is able to control the helicopter hovering at a desired $x$, $y$, $z$ position. Then, sinusoidal tracking is tested for the $z$-position, while $x$ and $y$ positions reach constant references.

1. *PID controllers performance*: Figs. 7–9 depict roll, pitch and yaw attitude angles, respectively. In each figure, the respective angle tracks a square signal, while the other two angles have zero as reference. Each figure shows how attitude angles are strongly coupled.

Further, Fig. 10 presents attitude angles, each one with zero reference. The system is subjected to a disturbance consisting of white noise, acting as wind disturbance on each body axis, incepted at 50 s, with a maximum wind velocity of 1 m/s. It has little effect over the attitude angles.

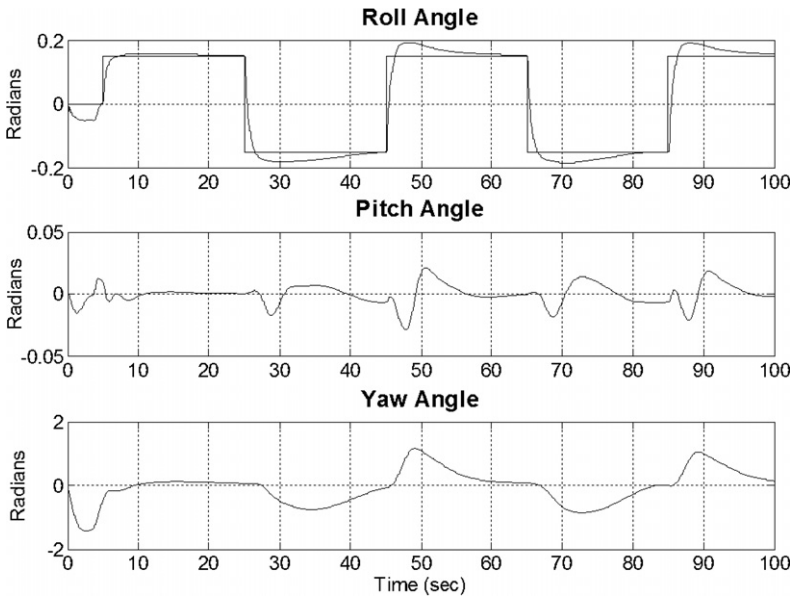


Fig. 7. Tracking a squared signal for roll angle.

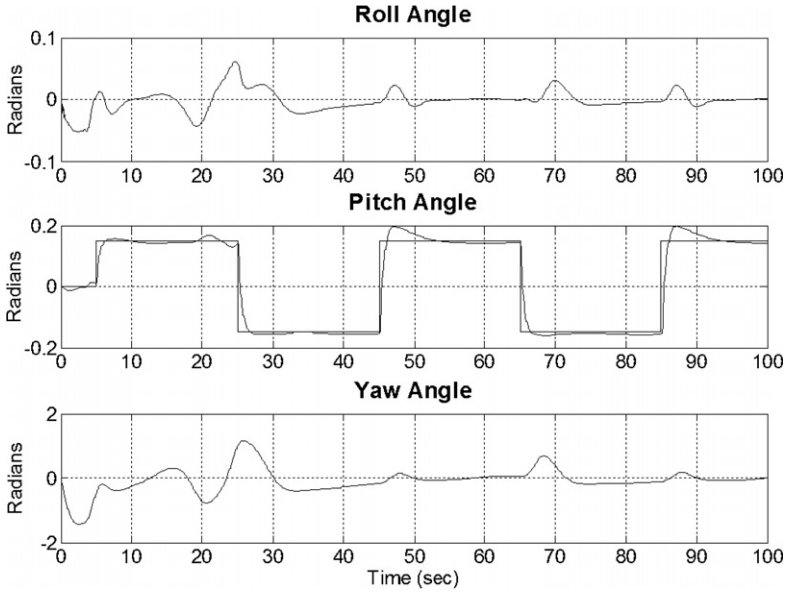


Fig. 8. Tracking a squared signal for pitch angle.

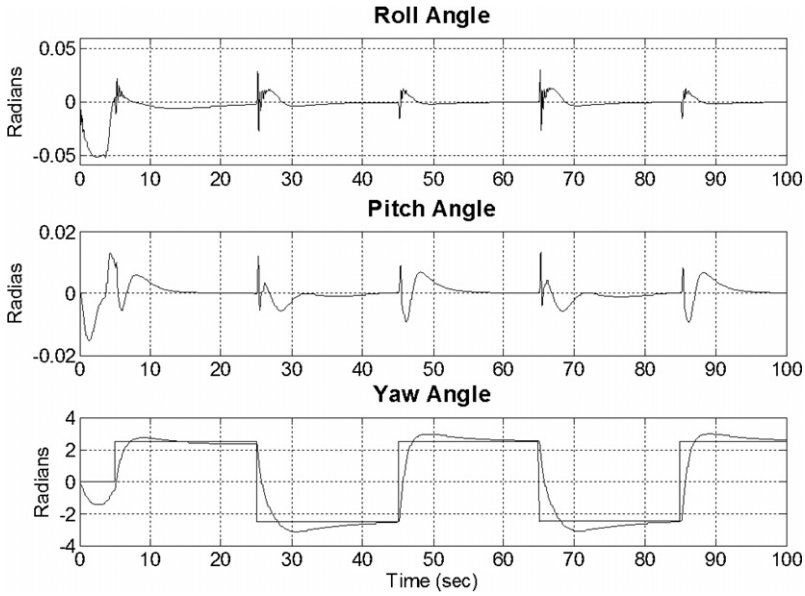


Fig. 9. Tracking a squared signal for yaw angle.

Finally, Fig. 11 shows the inertial position for the last attitude control condition, i.e., stabilization of attitude angles. It is shown as the $z$-position is taken to a 20 m reference. Note that the $x$- and $y$-positions increase fast.

2. *Fuzzy control performance*: Fig. 12 shows inertial position for the same previous condition, but now including fuzzy control. The $z$-position reaches a 20 m reference, and the $x$- and $y$-positions return to zero after a transient behavior.

Fig. 13 displays attitude angles for the previous 20 m $z$-reference, and the stabilization of $x$- and $y$-positions. Observe that the roll angle, $\phi$, and the pitch angle, $\theta$, are practically maintained at their trim values 0.07988

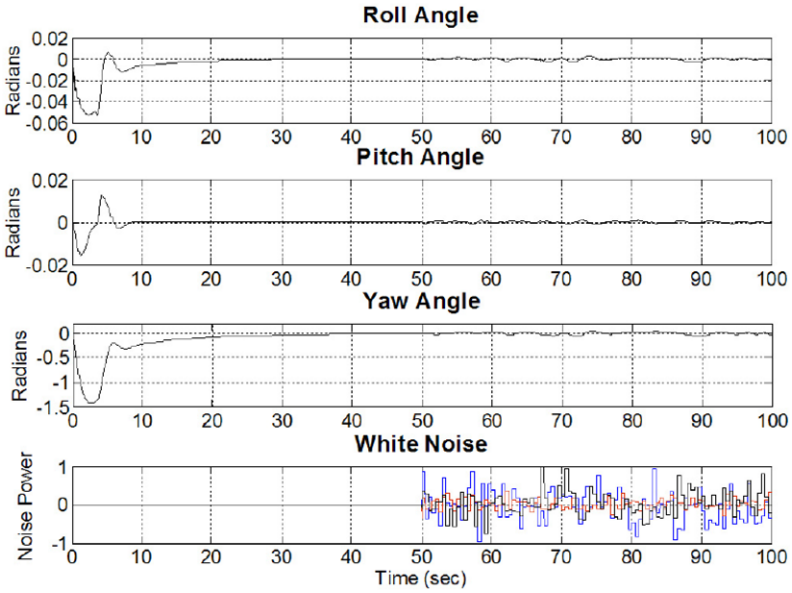


Fig. 10. Stabilization of attitude angles.

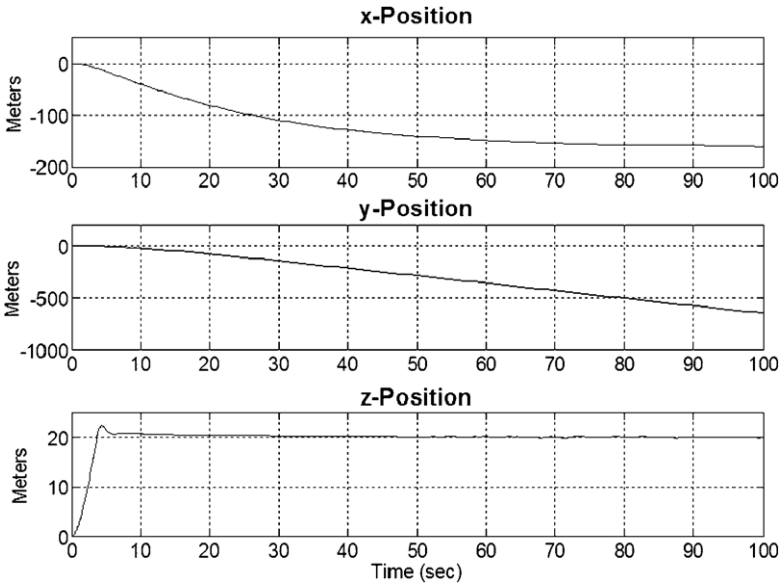


Fig. 11. $x$ and $y$-positions without control and tracking in $z$-position.

and 0, respectively. Due to the constant condition of position and attitude angles, the helicopter is maintained in hover flight.

3. *Position tracking*: Fig. 14 shows inertial position for constant tracking in $x$- and $y$-positions, and sinusoidal tracking in the $z$-position, with a good performance for the vertical ($z$) and longitudinal ($x$) movements. The angular frequency of the signal tracked by $z$ is 0.1 rad/s, and the $x$ reference is $-8$ m. Because of the coupling between collective input and lateral cyclic input, the $y$-position oscillates around the 5 m reference.

Fig. 15 presents attitude angles for the previous tracking condition. It is shown how roll and pitch angles oscillate to maintain the constant position. The yaw angle oscillates due to the coupling between the collective and pedals inputs.

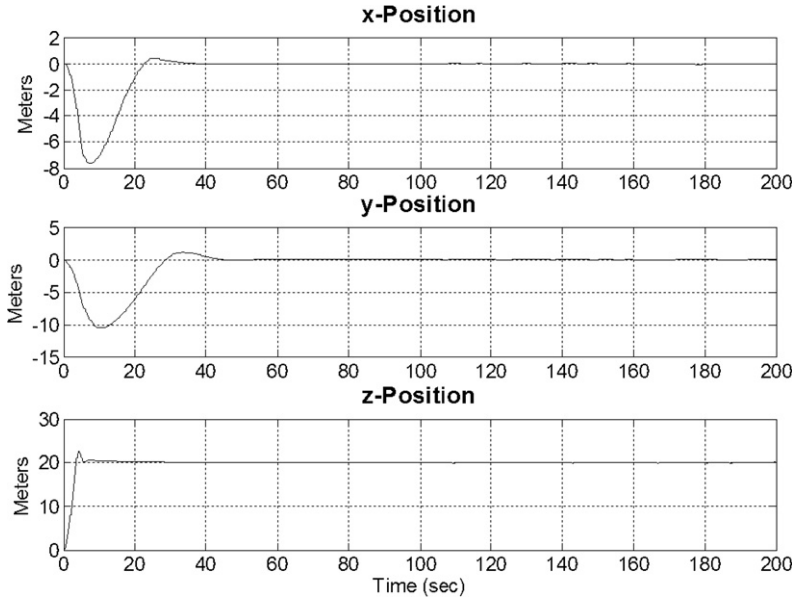


Fig. 12. Stabilization of inertial position.

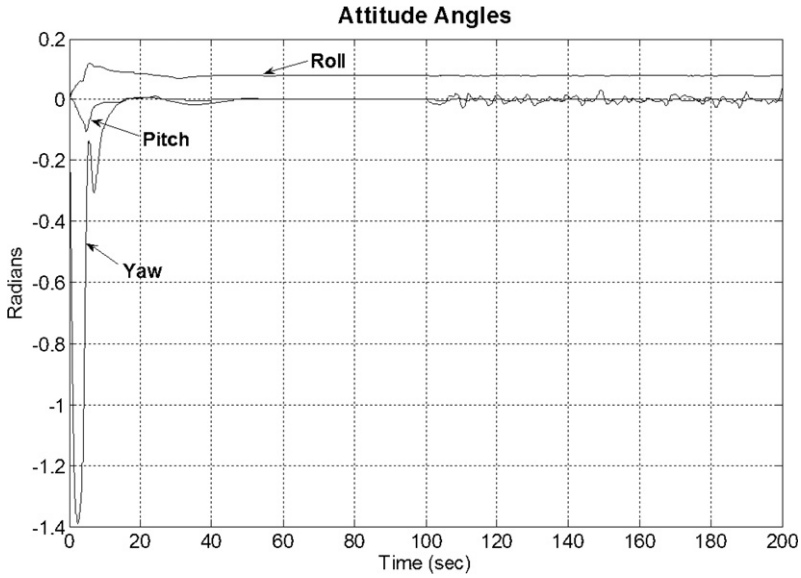


Fig. 13. Attitude angles to stabilization of positions.

Fig. 16 portrays control inputs for the previous condition. The cyclic inputs move sinusoidally to maintain the desired position, and also to react when the disturbance begins.

## 5. Combining fuzzy, PID and regulation control

Fig. 17 presents the detailed control scheme, in which fuzzy control, PID control and regulation theory are combined. The altitude/attitude control is composed of a MIMO linear regulator and two SISO PID controllers. The lateral/longitudinal control is constituted by two fuzzy controllers.

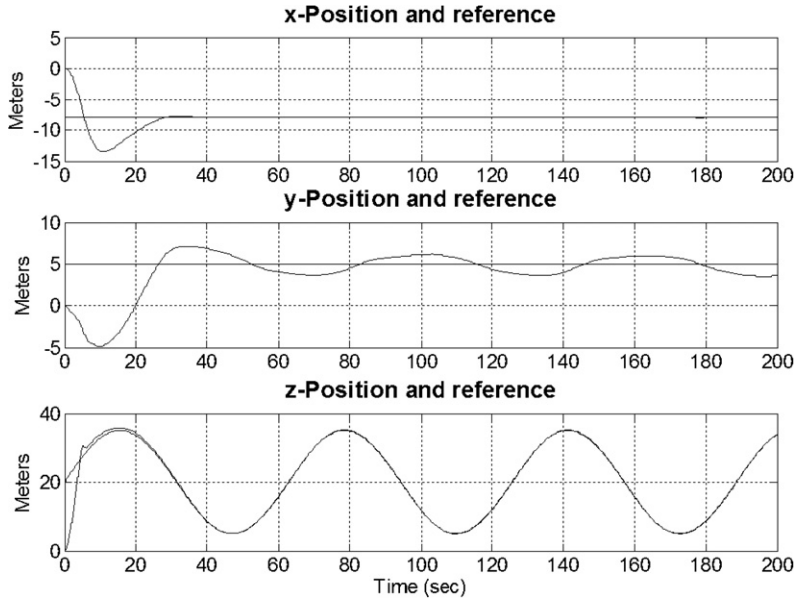


Fig. 14. Signal tracking for all the three positions.

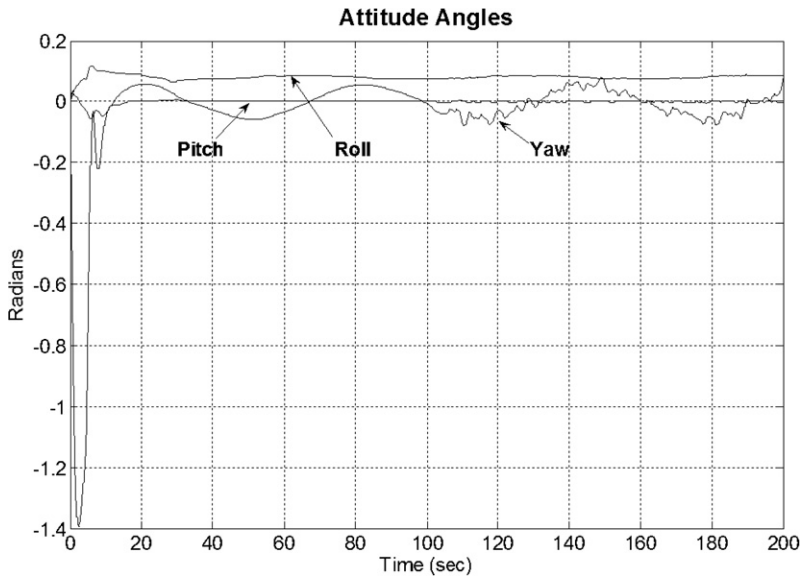


Fig. 15. Attitude angles to track references for all the three positions.

For this control scheme, we used several modules that were designed for the previous control scheme: the two Mamdani-type fuzzy controllers and the roll and pitch PID controllers. Thus, we only describe the regulator design.

### 5.1. Linear regulator

In linear regulator theory [2,9], the control goal is to obtain a stable closed-loop system and an asymptotic tracking error, for every possible initial state, and every possible exogenous input in a prescribed family of

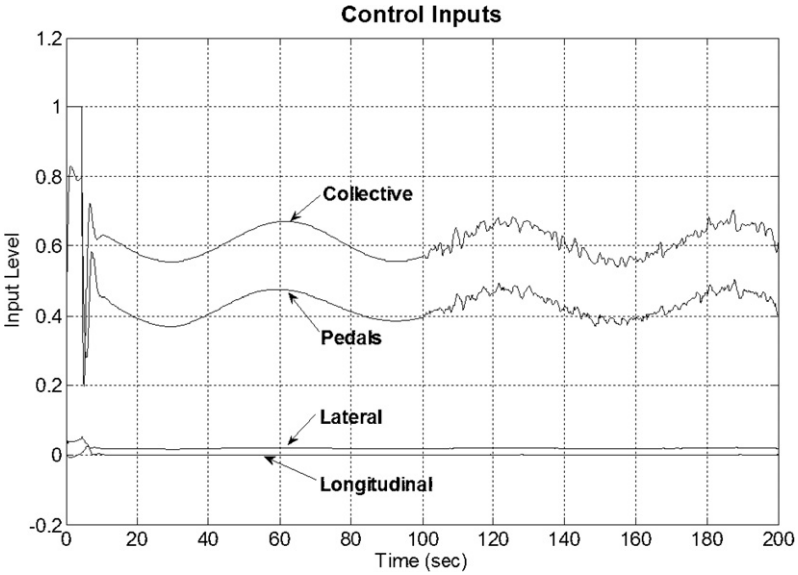


Fig. 16. Control inputs to track signals for all the three positions.

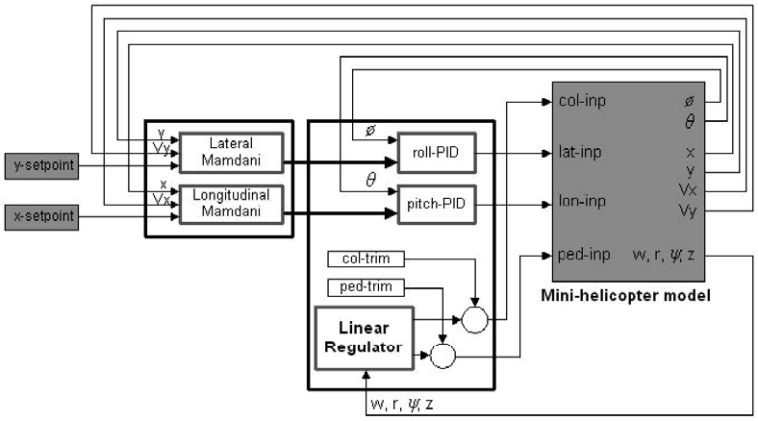


Fig. 17. Detailed scheme for combining fuzzy, PID and regulation control.

functions of time. This latter requirement is also known as the property of "output regulation". Consider a linear system

$$\begin{aligned} \dot{x}(t) &= Ax(t) + Bu(t) + Pw(t) \\ \dot{w}(t) &= Sw(t) \\ e(t) &= Cx(t) + Qw(t) \end{aligned} \tag{10}$$

where $x(t)$ is the internal state vector of the plant; $u(t)$ is the control input vector; $w(t)$ is the vector containing external disturbances and/or references; and $e(t)$ is the tracking error.

To solve this problem, the following hypotheses are assumed [2]:

(H1) the pair $(A, B)$ is stabilizable.

(H2) the exosystem $\dot{w}(t) = Sw(t)$ is antistable, i.e., all the eigenvalues of $S$ have a nonnegative real part.

Assuming (H1) and (H2) are satisfied, the problem of output regulation via state feedback can be determined if, and only if, there exist matrices $\Pi$ and $\Gamma$, which solve the following linear matrix equations:

$$\begin{aligned} \Pi S &= A\Pi + B\Gamma + P \\ 0 &= C\Pi + Q \end{aligned} \tag{11}$$

The necessary control law is given as $u(t) = Kx(t) + (\Gamma + K\Pi)w(t)$, with $K$ any matrix, such that $(A + BK)$ is Hurwitz. Defining $L = \Gamma + K\Pi$ we have

$$u(t) = Kx(t) + Lw(t) \tag{12}$$

In order to linearize the model presented in Section 2 using Matlab, it is necessary to use an adaptive process. Some assumptions have to be made, namely constant mass, constant rotor speed, and no dynamics for the actuators. Also, the rotational kinematics of motion have to be implemented as (7), i. e., quaternions are not used for linearization. Thus, the model to be linearized has fourteen states. We linearize it for hover flight. The values for this operation point are: $u = 0$; $v = 0$; $w = 0$; $p = 0$; $q = 0$; $r = 0$; $\phi = 0.07988$; $\theta = 0$; $\psi = 0$; $x = 0$; $y = 0$; $z = 20$; $a_1 = 0$; $b_1 = 0.007667$; $\delta_{\text{col}} = 0.6083$; $\delta_{\text{lon}} = 0$; $\delta_{\text{lat}} = 0.01902$; $\delta_{\text{ped}} = 0.4247$.

The resultant linear system is $\dot{\bar{x}} = A\bar{x} + B\bar{u}$, where $\bar{x} \in R^{14}$ , $\bar{u} \in R^4$, $A \in R^{14\times 14}$ and $B \in R^{14\times 4}$. This system is controllable, and it has a special characteristic: it is always the same for any $x$, $y$, $z$ position. This enables the system to achieve trajectory tracking for altitude, without the necessity of a linear controllers combination, which is required for the Takagi–Sugeno fuzzy approach.

In spite of the system being controllable, it is not possible to design a regulator for the complete system, due to the fact that the Francis equation (11) do not have suitable solutions either for $\phi$, $\theta$, $\psi$, and $z$, or for $x$, $y$, $z$, and $\psi$. Moreover, a regulator for $\phi$, $\theta$, $\psi$, and $z$ cannot maintain a desired position. This is only achieved by changing $\phi$ and $\theta$ in a suitable way. Hence, we design a regulator for a reduced linear system

$$\frac{\mathrm{d}\widehat{x}}{\mathrm{d}t} = A_r\,\widehat{x} + B_r\,\widehat{u} + P_{kn}\,\widehat{y} = C_r\,\widehat{x} \tag{13}$$

with $\widehat{x} = [\,w \quad r \quad \psi \quad z\,]^{\mathrm{T}}$, $\widehat{u} = [\,\delta_{\text{col}} \quad \delta_{\text{ped}}\,]^{\mathrm{T}}$, $\widehat{y} = [\,\psi \quad z\,]^{\mathrm{T}}$ and

$$A_r = \begin{bmatrix} -0.7985 & 0 & 0 & 0 \\ 0 & -0.8290 & 0 & 0 \\ 0 & 0.9986 & 0 & 0 \\ 0.9986 & 0 & 0 & 0 \end{bmatrix}$$

$$B_r = \begin{bmatrix} -21.0812 & 0 \\ 0 & 43.5170 \\ 0 & 0 \\ 0 & 0 \end{bmatrix}; \quad C_r = \begin{bmatrix} 0 & 0 & 1 & 0 \\ 0 & 0 & 0 & 1 \end{bmatrix} \tag{14}$$

where $P_{kn}$ is the disturbance vector due to the state variables, which are not considered in the reduced system. The elements of $P_{kn}$ can be considered as known disturbances, but only the first two disturbances fulfill the matching condition. However, the whole disturbance vector has a small contribution to the dynamic, and it is neglected.

For the linear system (13), we obtain a good performance with the following eigenvalues placement [7]:

$$[\,-0.5 \quad -12 \quad -10 \quad -1\,]$$

We propose to track a sinusoidal signal for altitude and a zero reference for yaw angle. The sinusoidal signal is defined as

$$f_{\text{ref}}(t) = P_{\text{const}} + P_{\text{am}}\sin(\alpha t) \tag{15}$$

where $P_{\text{const}}$ is the signal offset, $P_{\text{am}}$ is the signal amplitude, and $\alpha$ is the angular frequency in rad/s.

In order to generate $f_{\text{ref}}(t)$, we use the following dynamic system (exosystem):

$$\begin{bmatrix} \dot{\tilde{w}}_1 \\ \dot{\tilde{w}}_2 \\ \dot{\tilde{w}}_3 \end{bmatrix} = \begin{bmatrix} 0 & 0 & 0 \\ 0 & 0 & \alpha \\ 0 & -\alpha & 0 \end{bmatrix} \cdot \begin{bmatrix} \tilde{w}_1 \\ \tilde{w}_2 \\ \tilde{w}_3 \end{bmatrix} \tag{16}$$

with $[\,\tilde{w}_1(0) \quad \tilde{w}_2(0) \quad \tilde{w}_3(0)\,]^{\mathrm{T}} = [\,1 \quad 0 \quad 1\,]^{\mathrm{T}}$.

Thus, $f_{\text{ref}}(t)$ can be expressed as a linear combination of the state variables of the system (16)

$$f_{\text{ref}}(t) = P_{\text{const}}\tilde{w}_1 + P_{\text{am}}\tilde{w}_2$$

The resultant matrices for the regulator with $P_{\text{const}} = 20$, $P_{\text{am}} = 0$ are

$$\Pi = \begin{bmatrix} 0 \\ 0 \\ 0 \\ 20 \end{bmatrix}; \quad \Gamma = \begin{bmatrix} 0 \\ 0 \end{bmatrix}$$

The resultant matrices for the regulator with $P_{\text{cte}} = 20$, $P_{\text{am}} = 15$ and $\alpha = 0.1$ are

$$\Pi = \begin{bmatrix} 0 & 0 & -1.504815409 \\ 0 & 0 & 0 \\ 0 & 0 & 0 \\ 10 & 20 & 0 \end{bmatrix}; \quad \Gamma = \begin{bmatrix} 0 & -0.7138186675\mathrm{E}^{-2} & 0.5699842060\mathrm{E}^{-2} \\ 0 & 0 & 0 \end{bmatrix}$$

### 5.2. Simulation results

In this section, we discuss the performance for the overall control system for the case when the helicopter is forced to hover at a desired $x$, $y$, $z$ position. In addition, sinusoidal tracking is achieved for the $z$-position, while $x$- and $y$-positions reach constant references. Finally, a challenging test is performed by positioning the helicopter at equidistant points, which form a square in the $x$–$y$ plane. All the simulations are tested on

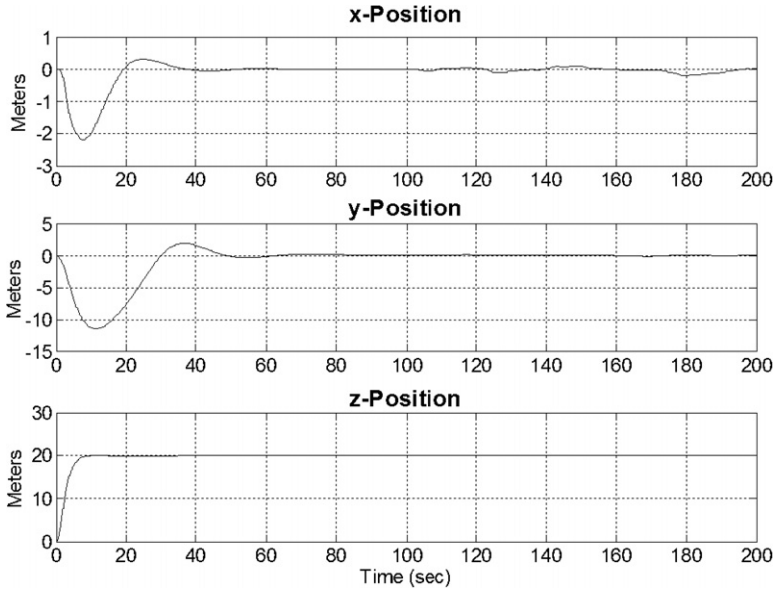


Fig. 18. Constant tracking for position.

the full mathematical model, which has decreasing mass, and non-constant rotor speed and dynamic for the actuators.

1. *Hover flight*: Fig. 18 shows inertial position for $P_{cte} = 20$ and $P_{am} = 0$. The $z$-position reaches a 20 m reference, and the $x$- and $y$-positions return to zero after a transient.

Fig. 19 displays attitude angles for the previous 20 m $z$-reference, and stabilization of $x$- and $y$-positions; roll angle, $\phi$, and pitch angle, $\theta$, are practically maintained on their trim values 0.07988 and 0, respectively. In this simulation, the system is subjected to white noise, which acts as a wind disturbance on each body axis., This disturbance is introduced at 100 s, with a maximum value velocity of 1 m/s, and has little effect over the attitude angles.

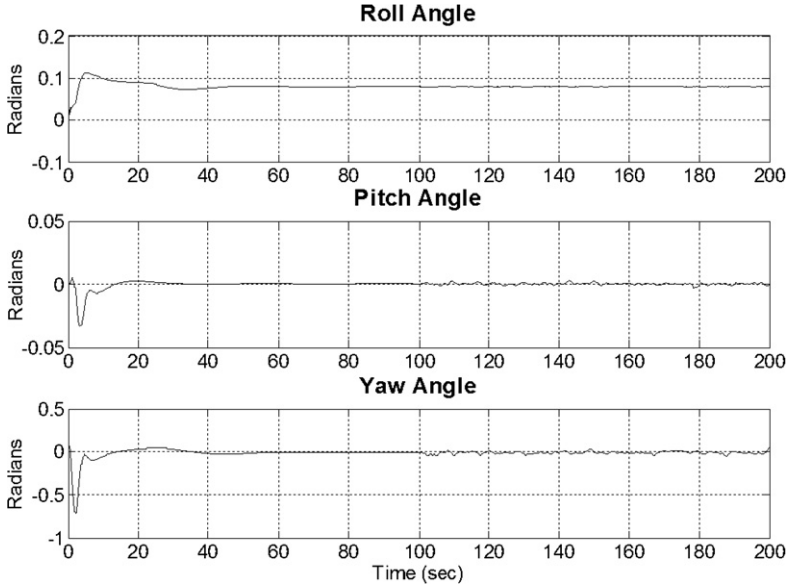


Fig. 19. Attitude angles to stabilization of positions.

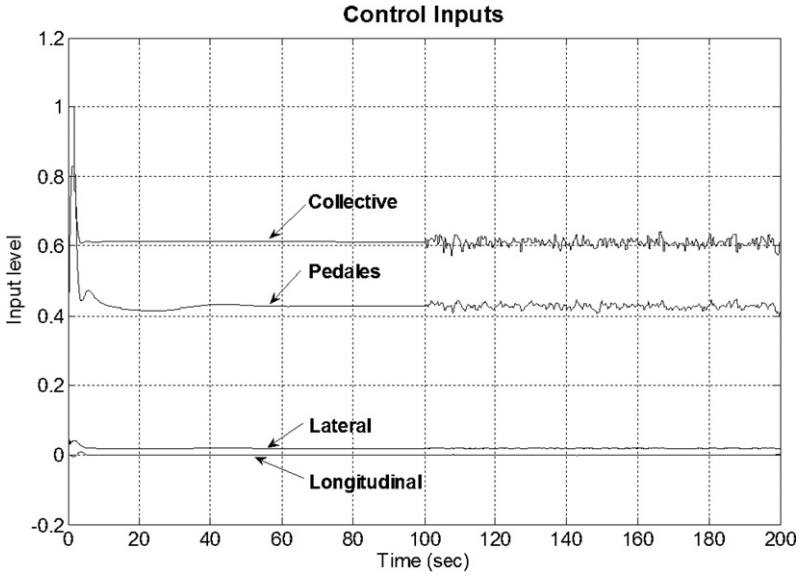


Fig. 20. Control inputs to stabilization of positions.

The helicopter reaches a steady condition for position and attitude angles, thus it is maintained in hover flight. Fig. 20 presents the control inputs to stabilize the three-dimensional position.

2. *Tracking for altitude*: Fig. 21 shows the inertial position for constant tracking in $x$- and $y$-positions, and sinusoidal tracking in $z$-position. We have $P_{\text{cte}} = 20$, $P_{\text{am}} = 15$ and $\alpha = 0.1$. The $x$-reference is $-8$ m and $y$-position has a 5 m constant reference. The controller has a good performance for the vertical ($z$) and longitudinal ($x$) movements. However, due to the coupling between collective input and lateral cyclic input, the $y$-position oscillates around its reference.

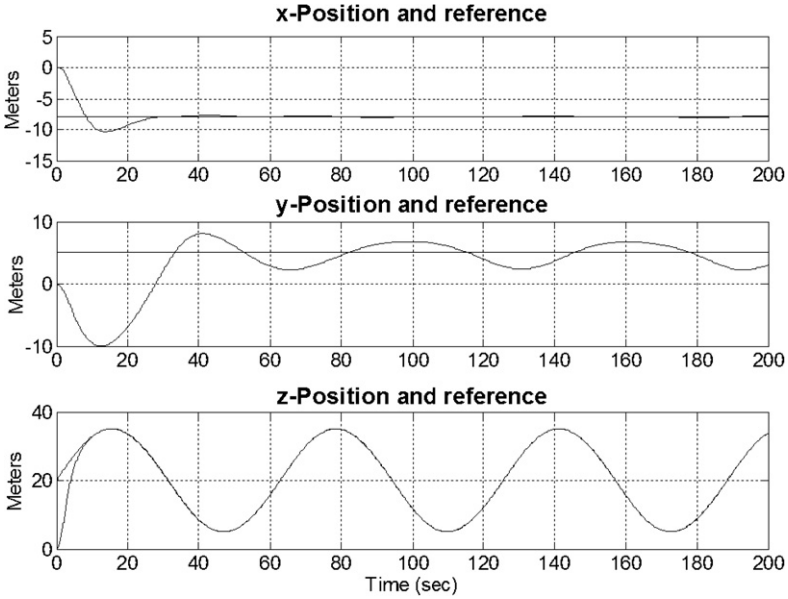


Fig. 21. Signal tracking for all the three positions.

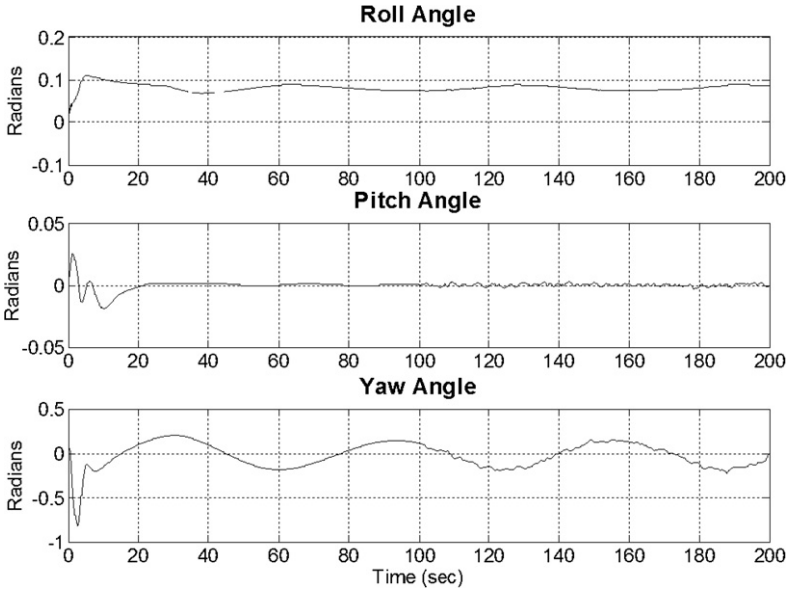


Fig. 22. Attitude angles to track signals in all the three positions.

Fig. 22 portrays attitude angles for the previous tracking condition. It is shown how roll and pitch angles oscillate to maintain the constant position. The yaw angle oscillates due to the coupling between the collective and pedals inputs.

Fig. 23 presents the control inputs for the previous condition. Each input follows a sinusoidal signal to maintain the desired position, and also to react when the disturbance begins, at 100 s. As we mentioned above, the control scheme is tested using the whole mathematical model, which considers non-constant rotor speed; thus, rotor speed dynamic is displayed in Fig. 24 together with its input command (throttle command).

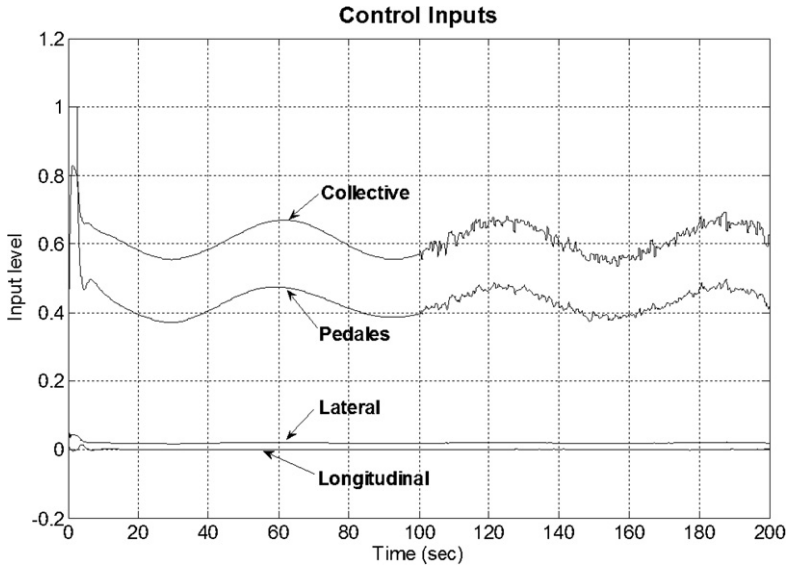


Fig. 23. Control inputs to track signals in all the three positions.

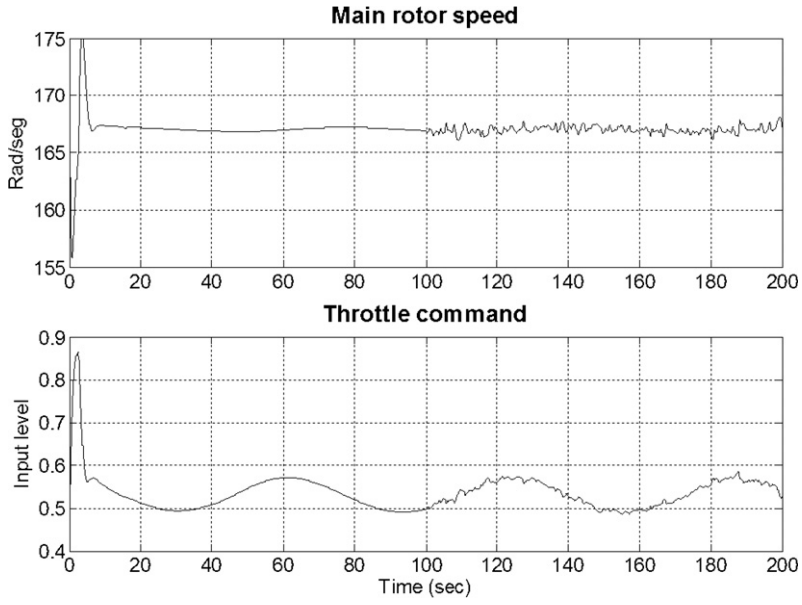


Fig. 24. Rotor speed and throttle command for tracking in altitude.

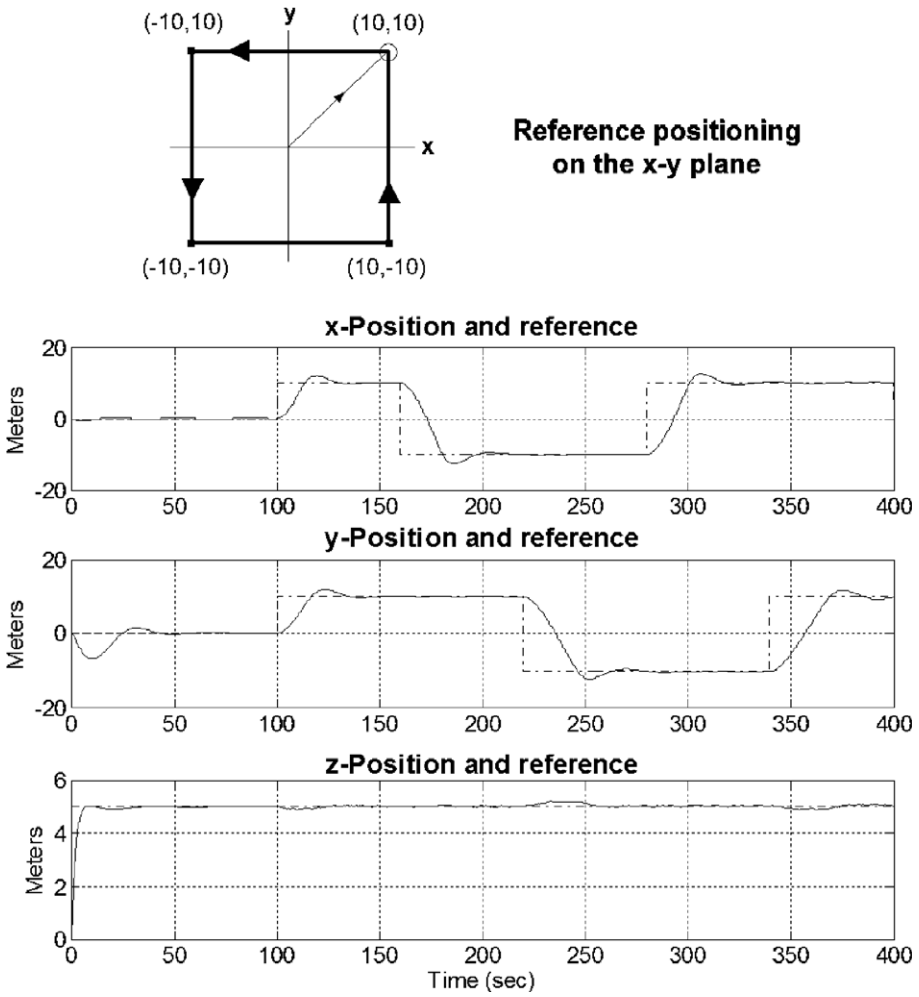


Fig. 25. Squared trajectory for motion on the $x$–$y$ plane.

3. *Positioning in x–y plane*: This last test consists of positioning the helicopter at equidistant points on the $x$–$y$ plane, which form a square, with vertices at $(10, 10)$, $(-10, 10)$, $(-10, -10)$ and $(10, -10)$. Fig. 25 displays this trajectory, which begins at $(0, 0)$. The altitude reaches a 5 m constant reference. We incepted a wind disturbance at 100 s. The dynamic for each position is slow; however, the helicopter always reaches the desired three-dimensional position.

Fig. 26 portrays the attitude angles required to reach the previous dynamic for the three-dimensional position. As shown, yaw angle is maintained close to zero, but it is slightly influenced by other dynamics, mainly due to the coupling between lateral input command and yaw angle. The four input commands applied to reach the desired positions are presented in Fig. 27.

**Comment 3.** The simulation results of this section show the well-behaved performance for the overall control system, even though the design procedure, decreasing mass, decreasing inertial moments, non-constant rotor speed and actuators' dynamics, are not considered.

**Comment 4.** Comparing the two control schemes proposed in this work, it can be concluded that the second (fuzzy-PID-regulation) improves the altitude tracking for a sinusoidal signal. Table 2 presents the corresponding values of the mean squared tracking error for both control schemes and for each controlled variable.

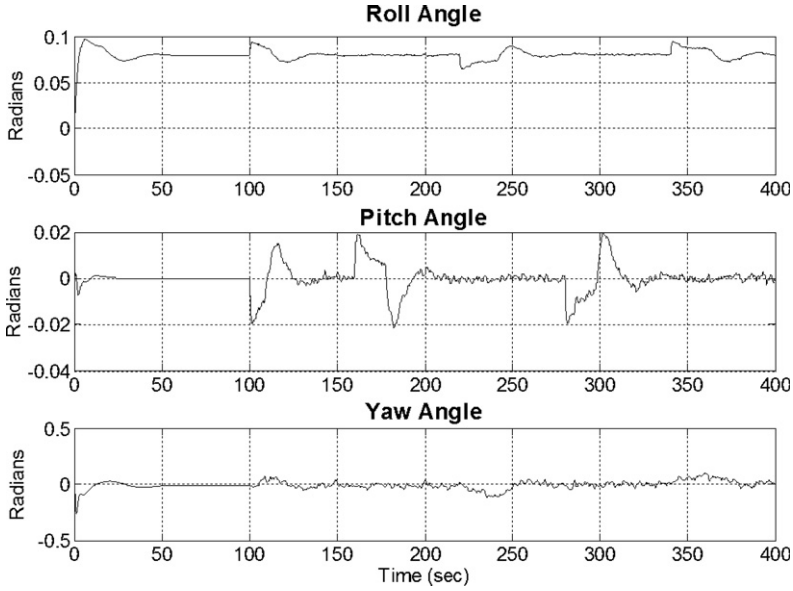


Fig. 26. Attitude angles to reach the squared trajectory on the $x$–$y$ plane.

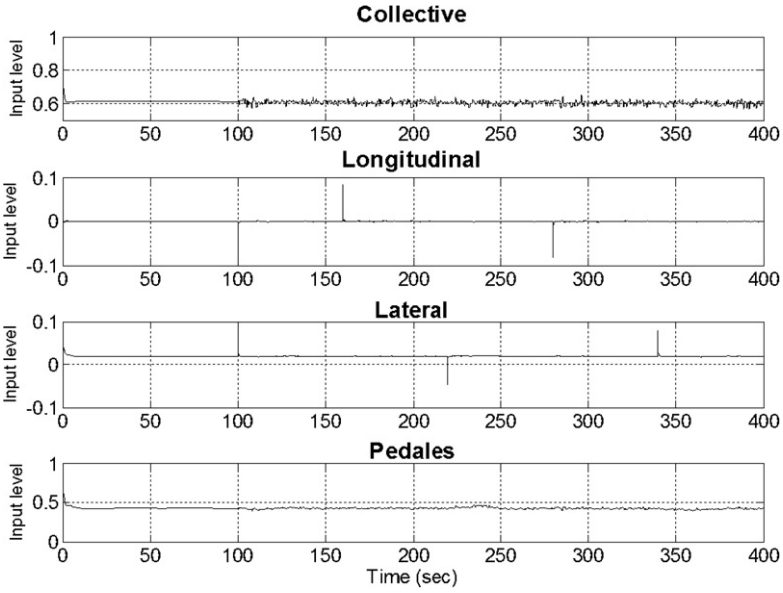


Fig. 27. Control inputs to reach squared trajectory on the $x$–$y$ plane.

Table 2
Mean squared tracking errors

| | Fuzzy-PID | Fuzzy-PID-regulation |
|---|---|---|
| Yaw angle | 0.0360 | 0.0217 |
| Altitude | 4.8045 | 4.8819 |

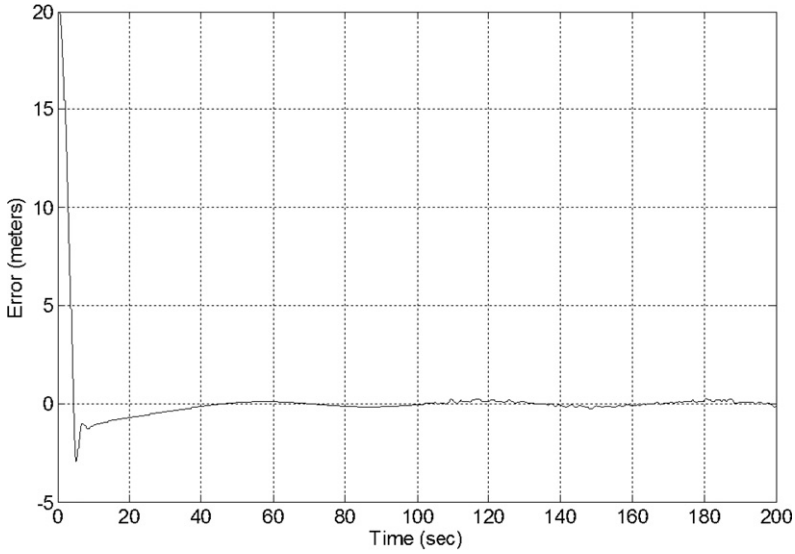


Fig. 28. $z$-Tracking error for fuzzy-PID control scheme.

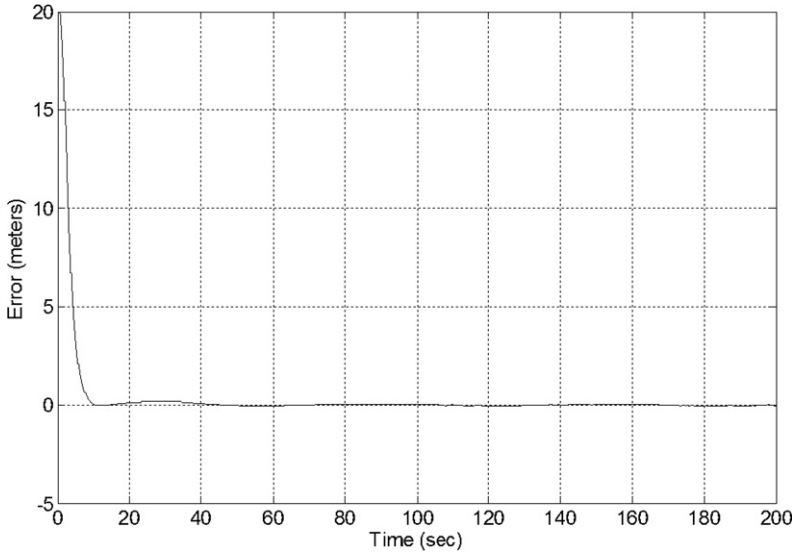


Fig. 29. $z$-Tracking error for fuzzy-PID-regulation control scheme.

Table 2 reveals that the fuzzy-PID-regulation scheme reduces the mean squared tracking error for the yaw angle, in comparison with the scheme obtained for the fuzzy-PID scheme. For altitude, the errors are similar. Figs. 28 and 29 display the $z$-tracking error for each scheme. They show that the fuzzy-PID-regulation controller performs better. The tracking error is practically eliminated, and the transient response is smaller than that of the fuzzy-PID scheme.

**Comment 5.** An extensive comparative analysis of our proposed control scheme with similar previously published works is not possible, due to the fact that there are very few publications presenting results regarding the tracking of time varying references for altitude. As far as we know, only [6] presents altitude trajectory tracking via simulation. Comparing our results with those of [6], the second scheme we propose is able to eliminate the altitude tracking error. Additionally, the fuzzy controllers in [6] are more complicated, since they use 25 rules, instead of the nine rules required by our schemes.

**Comment 6.** Finally, it is emphasized that the originality of this work is the development of simple and efficient control systems for a X-Cell mini-helicopter at slow velocity, using the more complex mathematical model currently known for this mini-helicopter. Simplicity is achieved with only four SISO PID controllers and two Mamdani controllers, which use only nine fuzzy rules – the minimum required quantity. Thus, the first proposed control scheme is the simplest control system for a mini-helicopter. Furthermore, an original idea presented in this work is the use of a reduced linear regulator – the second proposed control scheme – which controls only some dynamics of the system without decoupling. This is avoided with the use of Mamdani fuzzy-type controllers on the outer loop. This control scheme allows for the development of altitude tracking, using only one reduced linear model.

## 6. Conclusions

This paper outlines the design of hybrid intelligent control systems for a particular plant: the X-Cell mini-helicopter. The hybrid intelligent control systems are a combination of different control techniques, such as fuzzy logic, PID and regulation.

The general control scheme has an inner loop with an altitude/attitude control mode, and an outer loop, which controls translational motion. For both control systems the translational motion is controlled by two Mamdani fuzzy controllers. First, the fuzzy controllers are combined with PID controllers, to obtain an efficient system to stabilize the helicopter. Then, the fuzzy controllers are combined with PID and linear regulator controllers, which improves the performance for tracking signals in altitude without the necessity of the Takagi–Sugeno methodology.

Both hybrid intelligent control systems proposed in this work present good performance for hovering, positioning, and forward flight at slow velocities. Each system shows its effectiveness, via simulation, over the most realistic mathematical model currently used for a mini-helicopter. Moreover, both control systems offer the advantage of rapid implementation. As a part of the Colibri project, these systems are going to be implemented in real time.

In future work, we propose to deal with the coupling between dynamics, incorporating a velocity control system, and adding a fuzzy controller to compensate for the effect of changing yaw angle, which is kept equal to zero in this work.

## Acknowledgements

The authors are thankful for the support of Conacyt, Mexico, on project 39866Y, and of Colciencias, Colombia, on the Colibri project. They also thank the anonymous reviewers for helping to improve this paper.

## References

[1] K.J. Astrom, T. Hagglund, PID Controllers: Theory, Design, and Tuning, second ed., International Society for Measurement and Control, Research Triangle Park, NC, USA, 1995.
[2] B.A. Francis, The linear multivariable regulator problem, SIAM Journal on Control and Optimization 14 (1977) 486–505.
[3] V. Gavrilets, B. Mettler, E. Feron, Dynamic model for a miniature aerobatic helicopter, MIT-LIDS report, no. LIDS-P-2580, 2003.
[4] F. Hoffmann, T.J. Koo, O. Shakernia, Evolutionary design of a helicopter autopilot, in: Advances in Soft Computing: Engineering Design and Manufacturing, Part 3: Intelligent Control, Springer-Verlag, 1999, pp. 201–214.
[5] R. John, Soft computing and hybrid approaches: an introduction to this special issue, Information Sciences 150 (1–2) (2003) 1–3.
[6] B. Kadmiry, D. Driankov, A fuzzy flight controller combining linguistic and model-based fuzzy control, International Journal on Fuzzy Sets and Systems 146 (3) (2004).
[7] T. Kailath, Linear Systems, Prentice-Hall, Upper Saddle River, NJ, USA, 1980.
[8] T. Koo, S. Sastry, Output tracking control design of a helicopter model based on approximate linearization, in: Proc. 37th IEEE Conf. on Decision and Control (CDC'98), Tampa, FL, USA, December 1998, pp. 3635–3640.
[9] H.W. Knobloch, A. Isidori, D. Flockerzi, Topics in Control Theory, Birkhauser, Boston, MA, USA, 1993.
[10] P. Melin, O. Castillo, Intelligent control of aircraft dynamic systems with a new hybrid neuro-fuzzy-fractal approach, Information Sciences 142 (1–4) (2002) 161–175.

[11] B. Mettler, Identification Modeling and Characteristics of Miniature Rotorcraft, Kluwer Academic Publishers, Boston, MA, USA, 2003.
[12] K. Passino, S. Yurkovich, Fuzzy Control, Addison-Wesley–Longman, Menlo Park, CA, USA, 1998.
[13] C. Phillips, C.L. Karr, G. Walker, Helicopter flight control with fuzzy logic and genetic algorithms, Engineering Applications of Artificial Intelligence 9 (2) (1996) 175–184.
[14] J.V.R. Prasad, Anthony J. Calise, J. Eric Corban, Yubo Pei, Adaptive nonlinear controller synthesis and flight test evaluation on an unmanned helicopter, in: Proc. IEEE International Conference on Control Applications, Hawaii, USA, August 1999.
[15] H. Shim, T.J. Koo, S. Sastry, A comprehensive study of control design for an autonomous helicopter, in: Proc. 37th IEEE conference on Decision and Control, Tampa, Florida, USA, December 1998, pp. 3653–3658.
[16] M. Sugeno, Development of an intelligent unmanned helicopter, in: M. Sugeno, T.H. Nguyen, N.R. Prasad (Eds.), Fuzzy Modeling and Control, Selected Works, CRC Press, Boca Raton, FL, USA, 1999, pp. 13–43.
[17] L.X. Wang, A Course in Fuzzy Systems and Control, Prentice Hall, Upper Saddle River, NJ, USA, 1997.
[18] T. Yamaguchi, K. Goto, T. Takagi, Two-degree-of-freedom fuzzy model using associative memories and its applications, Information Sciences 71 (1–2) (1993) 65–97.
[19] www.control-systems.net/colibri.htm.